Published in final edited form as:

Biomaterials. 2017 January ; 114: 1–9. doi:10.1016/j.biomaterials.2016.10.049.

Local pulsatile PTH delivery regenerates bone defect via enhanced bone remodeling in a cell-free scaffold

Ming Dang[a], **Amy J. Koh**[b], **Xiaobing Jin**[d], **Laurie K. McCauley**[b], and **Peter X. Ma**[a,c,d,e,*]

[a]Macromolecular Science and Engineering Center, University of Michigan, Ann Arbor, MI, 48109-1078

[b]Department of Periodontics and Oral Medicine, University of Michigan School of Dentistry, Ann Arbor, MI 48109

[c]Department of Biologic and Materials Sciences, University of Michigan, Ann Arbor, MI, 48109-1078

[d]Department of Biomedical Engineering, University of Michigan, Ann Arbor, MI, 48109-1078

[e]Department of Materials Science and Engineering, University of Michigan, Ann Arbor, MI, 48109-1078

Abstract

Parathyroid hormone (PTH) is currently the only FDA-approved anabolic drug to treat osteoporosis, and is systemically administered through daily injections. A new local pulsatile PTH delivery device was developed from biodegradable polymers to expand PTH's application from osteoporosis treatment to spatially controlled local bone defect regeneration in this work. This is the first time that local pulsatile PTH delivery has been demonstrated to promote bone regeneration via enhanced bone remodeling. The biodegradable delivery device was designed to locally deliver PTH in a preprogrammed pulsatile manner. The PTH delivery was utilized to facilitate the regeneration of a bone defect spatially defined with a cell-free biomimetic nanofibrous (NF) scaffold. The local pulsatile PTH delivery (daily pulse for 21 days) not only promoted the regeneration of a critical-sized bone defect with negligible systemic side effects in a mouse model, but also advantageously achieved higher quality regenerated bone than the standard systemic PTH injection. These results demonstrate a promising and novel pulsatile PTH delivery device for spatially defined local bone regeneration.

Keywords

PTH; pulsatile release; cell-free; 3D scaffold; bone remodeling; bone regeneration

[*]Corresponding author. mapx@umich.edu.
Current address: 1011 North University Ave., Room 2209, The University of Michigan, Ann Arbor, MI 48109-1078, USA

1. Introduction

In the past decade, significant progress has been made in developing scaffolds, discovering growth factors, and identifying progenitor and stem cells in the field of bone tissue engineering [1, 2]. To robustly regenerate high quality bone often requires the addition of cells, but the cell-based therapies suffer major limitations such as the source of cells, the in vitro manipulation, rigorous regulatory approval process and associated high costs [3, 4]. Acellular biomaterials are emerging to overcome the need for addition of external cells for tissue regeneration. Such cell-free approaches require advanced biomimetic material design, drawing on biological knowledge and engineering tools, to create microenvironments that favorably interact with local tissues and cells to orchestrate the regeneration processes [5–7].

Drug delivery strategies are utilized to induce and accelerate bone formation in acellular biomaterials [8]. A variety of osteoinductive molecules (small molecules [9, 10], proteins [8, 11, 12], DNAs [13, 14], RNAs [3], etc.) have been investigated for their ability to induce and accelerate bone regeneration. However, most of them frequently fail in translational trials due to side effects resulting from the supraphysiological drug concentrations needed to achieve the desired repair. More importantly, such osteoinductive molecules could lead to undesired ectopic bone formation or bone overgrowth, due to a lack of bone remodeling in the regenerated bone tissue [15].

Parathyroid hormone (PTH) is well known to stimulate bone remodeling and can lead to either bone loss or bone gain depending on the balance between bone resorption and formation. Continuous exposure of PTH increases osteoclast activity resulting in bone resorption, whereas intermittent administration of PTH promotes osteoblast activity (bone formation) to a higher degree than osteoclast activity (bone resorption), thus resulting in net bone formation [16, 17]. The anabolic application of PTH is currently a FDA-approved treatment for osteoporosis by systemically strengthening bone [18–20]. However, extending PTH utilization from systemic treatment for osteoporosis to localized application for bone defect regeneration has not been achieved. The major drawbacks of repurposing PTH as a therapeutic for local defect repair include its unintended systemic side effect and its administration via daily injection, which is inconvenient for patient compliance. Many different drug delivery strategies have been investigated but most center on systemic administration [20]. Successful systems to deliver PTH to the local site, to preserve PTH bioactivity and to induce the optimal anabolic action are lacking.

In this work, we developed a novel acellular biomaterial strategy to promote bone regeneration by incorporating local PTH delivery in a 3D biomimetic scaffold (Fig. 1). Biodegradable drug delivery devices were designed to preprogram the delivery of PTH in either a pulsatile or continuous manner for 21 days using a surface erosion polyanhydride (PA). We investigated the effects of the two distinct kinetics, pulsatile and continuous, in a local calvarial defect regeneration model. Such platform allowed us to explore the potential of PTH for the treatment of localized bone defects.

2. Materials and methods

2.1 Materials

Three-component PA was synthesized by polymerizing sebacic acid (SA), 1,3-bis (p-carboxyphenoxy) propane (CPP), and poly(ethylene glycol) (PEG, MW=1000 Da) as previously reported [21]. Poly(l-lactic acid) (PLLA, Resomer L207S) with an inherent viscosity of 0.8~1.2 dl/g (0.1 % in chloroform, 25 °C) was purchased from Boehringer Ingelheim (Ingelheim, Germany). PTH (1–34), was obtained from Bachem Bioscience Inc (Torrance, CA). SA, CPP, PEG, polycaprolactone (PCL), polyvinyl alcohol (PVA), bovine serum albumin (BSA), alginate, gelatin, fructose, mineral oil, tetrahydrofuran (THF) and dichloromethane (DCM) were purchased from Sigma-Aldrich Company (USA) and used as received. Phosphate-Buffered Saline (PBS) was purchased from Life Technologies Company (USA).

2.2 3D Nanofiberous (NF) scaffold

3D NF PLLA scaffolds with inter-connected spherical pores were fabricated as previously described [22]. Briefly, fructose sugar spheres were made by emulsion technique. 50 g fructose was melted at 130 °C into clear light yellowish liquid and the liquefied sugar was gradually added into 50 mL mineral oil with 1.5 mL Span 80 under vigorous stirring for 3 minutes to create emulsion. The mixture was cooled down in an ice-bath to solidify the sugar spheres and sifted with standard sieves to separate them by size. Spheres of desired-size (250–420 μm) were collected, washed with hexane for three times, and added to a Teflon mold. The mold was heat-treated at 37 °C for 15 minutes to achieve the desired interconnected pore structure. After bonding the sugar spheres, hexane was removed under vacuum. PLLA/THF (10% w/v solution) was then cast into the sugar sphere assembly and the whole construct was stored at −80 °C over night to induce phase separation. The phase-separated samples were immersed into distilled water to extract the solvent and leach away the sugar spheres. Last, the polymer scaffolds were freeze-dried and punched into desired size (2.3 mm in diameter and 1.5 mm in thickness).

2.3 PTH pulsatile delivery device

To fabricate pulsatile devices, the PA (weight ratio: SA-CPP-PEG=80-20-2) was melted and hot compressed into films of 50 μm in thicknesses with an error of ±5 μm. PTH/Alginate mixture (1:1.67 weight ratio) was dissolved in distilled water and the solution was cast into films and freeze-dried to obtain drug films. The PA films were punched into disks of 3 mm in diameter and the drug films were punched into disks of 1.5 mm in diameter. The PA disks were rubbed against a Teflon film to generate positive charge on the PA disks and the drug disks were rubbed against a glass slide to generate negative charge on the drug disks. We used non-contact static meter (Electro-Tech Systems Static Meter Model 200) to determine the charges generated on both films and we found +(157± 67) mV on the PA film and –(80±30) mV on the drug film. One piece of positive PA disk and one piece of negative drug disk attracted to each other to form a bilayer and the 21 bilayers were then stacked to obtain a layer-by-layer construct. The bottom and side of the construct were sealed with a 35% w/v PCL/DCM solution, leaving the top unsealed. To calculate the PTH loading efficiency, PTH-loaded devices were hydrolyzed by a mixture of 0.5 ml of 1 M NaOH and 0.5 ml PBS with

shaking at room temperature for 2 hours. After hydrolysis, 0.5 ml of 1 M HCl was added to neutralize the sample solutions. The samples were centrifuged at 3000 rpm for 5 minutes and the supernatant samples were collected. Protein amounts in the supernatant were determined by MicroBCA method (Pierce, Rockford, IL). The loading efficiency was determined by dividing the retained PTH amount over initially loaded PTH amount.

2.4 PTH continuous delivery device

To fabricate the continuous delivery device, a double emulsion method [23] was employed to prepare PTH-loaded PA (weight ratio: SA-CPP-PEG=80-20-2) microspheres. 200 μl PTH solution was emulsified into 1 ml 10 % w/v PA polymer DCM solution, using a probe sonicator at an output power of 10 W (Virsonic 100, Cardiner, NY) for 20s over an ice bath to create a water-in-oil (w/o) emulsion. The w/o emulsion was then added into 20 ml PVA aqueous solution (1% w/v) under sonication at an output power of 20 W to create a water-in-oil-in-water (w/o/w) double emulsion. The solution was stirred at room temperature for 3 hours to evaporate DCM and then centrifuged at 6000 rpm for 6 minutes to collect solid microspheres. The microspheres were washed with distilled water three times and freeze dried. The freeze-dried microspheres were then compressed into disks of the same size as the pulsatile device. The bottoms and sides of the disks were sealed with a 35% w/v PCL/DCM solution. The particles size and polydispersity were measured by Dynamic Light Scattering (DLS) particle analyzer (DelsaTM Nano C, Beckman Coulter). To calculate the PTH encapsulation efficiency, 5 mg PTH-loaded PA microspheres were hydrolyzed to measure the amount of the protein encapsulated, using the same procedure as the pulsatile device. The encapsulation efficiency was determined by dividing the retained PTH amount over initially loaded PTH amount.

2.5 Scanning electron microscopy (SEM) observation

The pulsatile and continuous PTH release devices were cut in the middle by a sharp blade. The cross sections of the two devices and the PLLA scaffold were coated with gold. The morphology of the materials was examined using Scanning Electron Microscopy (SEM) (JEOL 7800FLV, USA).

2.6 In vitro PTH Release and PTH Bioactivity

The PTH-loaded devices were immersed in 1 ml PBS (0.1 M, pH = 7.4) and incubated at 37 °C. The medium were collected at designated time points and replaced with equal amount of fresh PBS. The samples were stored at −80 °C until analysis. The amount of released PTH was measured using PTH ELISA kit (Immutopics, Inc) [24]. The bioactivity of released PTH was determined using the adenylate cyclase stimulation assay and cAMP-binding protein assay as described previously [23].

2.7 Calvarial bone-defect repair model construction

All animal procedures were performed following a protocol approved by the University of Michigan Institutional Animal Care and Use Committee. C57BL/6 mice were randomly divided into four groups. Animals were anaesthetized with isoflurane (2%) inhalation. A 2.3 mm craniotomy defect centered on the parietal calvarial bone was created using a trephine.

A blank scaffold was placed to fill in the defect and a delivery device (pulsatile PTH, continuous PTH or BSA control) was placed adjacent to the scaffold with the opening side facing the scaffold. The PTH injection group did not receive PTH delivery devices; instead subcutaneous injection of PTH (40 μg/kg/d) was administrated for 21 days.

The mice were euthanized 8 weeks after implantation. The skull and tibiae were harvested.

2.8 Micro CT analysis

For the calvarial bone analysis, the skulls were scanned with a fixed global threshold of 20%. 3D reconstruction of the skull and quantitative analyses were performed. A 2.3 mm-round region of interest centered on the defect was determined and the bone volume (mm^3) (BV) and bone mineral density (BMD) in the area were measured using manufacturer's software (Scanco μCT 100).

For the tibiae analyses, tibiae were scanned over the entire length. A fixed global threshold of 18% (180 on a grayscale of 0–1000) was used to segment trabecular bone from non-bone areas. A region of 0.75mm right below the growth plate was analyzed to quantify the trabecular bone volume.

2.9 Bone histological and histomorphometric analysis

The calvarial samples were fixed with 4% formalin, decalcified with 10% EDTA for 2 weeks and subsequently embedded in paraffin. Hematoxylin & eosin (H&E) staining of the coronal sections (5 μm thick) were performed by the histology core at the University of Michigan School of Dentistry. Tartrate-resistant acid phosphatase (TRAP) staining was performed using the Leukocyte Acid Phosphatase Assay (Sigma) following the manufacturer's protocol. Bone static histomorphometric analyses for bone area and osteoclast number were performed using a computer-assisted histomorphometric analyzing system (Image-Pro Plus version 4.0; Media Cybernetics, Inc., Silver Spring, MD).

2.10 Serum biomarker analysis

Three weeks after implantation, the mice were anaesthetized with inhalation of isoflurane (2%) and blood was collected by tail blood draw. After centrifuge for 10 mins at 13000rpm, serum was separated and kept frozen until biochemical assays were performed. Serum procollagen I N-terminal propeptide (P1NP) (MyBioSource, Inc) and TRAP5b (Novatein Biosciences, MA) ELISA immunoassays were performed following the manufacturer's protocols.

2.11 Statistical analysis

All numerical data are presented as mean ± SD. All P values were two-tailed and $P<0.05$ was considered statistically significant. One-way ANOVA test was applied to compare different groups using GraphPad InStat software (GraphPad).

3. Results

3.1 3D Nanofibrous (NF) scaffold

The scaffold plays an important role in defining the 3D microenvironment for the regenerative cells. Pore size, porosity and surface architecture are important parameters to design an ideal scaffold for regeneration [1]. In this work, we combined the sugar spheres leaching technique with the thermal induced phase separation technique to fabricate NF PLLA scaffolds with inter-connected spherical pore network [22] (Fig. 2 A, B). The spherical pores of the scaffold ranged from 250 μm to 420 μm and the porosity was as high as 98.5%. The major organic component of bone is collagen, which self-assembles into nanofibers ranging from 50 to 400 nm in diameter [2] and the PLLA scaffold surface (inset in Fig. 2 B) had the similar NF feature of collagen.

3.2 PTH delivery devices

The two types of PTH delivery devices were fabricated to achieve pulsatile and continuous release for 21 days so as to determine the optimal PTH release kinetics for bone regeneration. For the pulsatile device, the PA was synthesized and hot pressed into thin films of desired thickness. PTH was mixed with alginate in PBS and casted into drug films. Alginate was used as a drug carrier due to its biocompatibility and processing properties [24]. Twenty-one PA isolation layers and twenty-one drug films were stacked alternatively using an electrostatic-assisted layer-by-layer assembly technique, which enabled close contact between isolation layers and drug layers and eliminated air gaps. The drug layers were designed to be smaller than the isolation layers in diameter, so that the chance of connection between drug films was decreased, preventing leakage of the drug at the point where it is most likely to happen (Fig. 2 C, D). The PTH loading efficiency of the pulsatile device was as high as 98.5% that PTH was well retained in the drug layers. For the continuous device, PTH with 1% w/v bovine serum albumin (BSA)/gelatin was encapsulated into PA microspheres using a double emulsion technique. The BSA/gelatin helped to protect the PTH from denaturing during the emulsion process [8]. The microspheres encapsulation efficiency was calculated to be 86.3 ± 3.2 %. The PTH-loaded microspheres of 3μm mean diameter and 0. 351 polydispersity were compressed into disks, the same size as the pulsatile devices (Fig. 2 E, F). The sides and bottoms of both types of devices were sealed with PCL, a slow degrading polymer, leaving only the top unsealed, thus allowing a unidirectional drug release from the opening top.

3.3 In vitro long-term release of PTH

The effect of PTH on bone was found to be dependent on the stage of development and 3-week daily PTH injection was found to exert prominent anabolic actions in an osteoregeneration model [25]. Therefore, the long-term (21 days) pulsatile PTH release was necessary to study bone regeneration against the continuous PTH release in a critical size defect repair model. The surface erosion rate of PA was found to vary with the chemical composition of the PA (PEG content and SA-CPP ratio) [21, 26]. For the pulsatile delivery device, PA is a typical surface erosion polymer and thus the “dissolution time” is proportional to the polymer layer thickness[24]. In this study, the average interval time between two adjacent PTH peaks exhibited a linear relationship with the thickness of

isolation layer and the linear regression equation is $\bar{T}(hour) = 0.26h(\mu m) + 7.5$. Twenty-one PA (SA-CPP-PEG=80-20-2) isolation layers with a thickness of 50 μm each were able to achieve the desired 21 daily pulses of release. The same PA (SA-CPP-PEG=80-20-2) was used to achieve continuous drug release for 21 days from the continuous release device. The *in vitro* PTH release profiles were determined using the PTH ELISA kit [27]. The ELISA data showed that using a pulsatile release device around 90% of the PTH was released in a pulsatile manner over the 21 days (Fig. 3A). Using the continuous release device nearly the same amount of PTH was released in a linear manner for 21 days (Fig. 3B).

In addition, the released PTH from both types of devices was collected every hour on days 1, 10 and 20. The bioactivity of the released PTH was determined using the adenylyl cyclase stimulation and cAMP binding assay [23]. The released bioactive PTH data showed that pulsatile PTH release devolved from a sharp peak (day 1) to a relatively broader peak (day 20) over time (Fig. 4 upper panel). This may be due to the increased diffusion distance of PTH through the residual PA layers. However, the pulsatile release feature was maintained over the 21 days. The bioactive PTH was released at a steady rate from the continuous device, which is consistent with the linear release behavior shown from the ELISA data (Fig. 4 lower panel).

3.4 Mouse calvarial bone defect repair

To determine the optimal PTH release mode to ensure desired PTH anabolic action in bone regeneration, the pulsatile device (21 layers) and the continuous device (21 days) were compared in identical experimental set ups to access the outcomes of bone regeneration in a critical size (2.3 mm in diameter) round defect created in the mouse skull. BSA loaded pulsatile devices were used as vehicle controls. In the positive control group, we injected PTH for 3 weeks using a standard systemic administration dose (40 μg/kg/d), which showed notable anabolic effects as reported before [27]. Both the pulsatile devices and continuous devices were loaded with the same amount of PTH as the total standard injection amount.

Eight weeks after implantation, μCT reconstruction of the skulls (Fig. 5 A) showed that local pulsatile PTH release resulted in the best regeneration outcome among all groups; whereas continuous PTH release resulted in less bone compared to the BSA control group. H&E (Fig. 6 A) and Trichrome staining (Fig. 6 B) showed that in the pulsatile PTH group, collagen-rich bone tissue (stained pink in H&E staining and dark blue in Trichrome staining) was formed throughout the scaffold, whereas only fibrous tissue was present in the continuous PTH group. Areas and volumes of newly formed bone were quantitatively analyzed using μCT and histomorphometry, revealing that the PTH injection significantly promoted bone growth in the NF scaffold compared to the control BSA group. Further, local pulsatile PTH release significantly increased bone volume and connected bone tissue regeneration even compared to systemic PTH injection (Fig. 5 B and Fig. 6 A).

TRAP staining (Fig. 6 C) and the resultant osteoclast analysis (Fig. 7 B, C) showed that both pulsatile and continuous PTH release devices increased the number of osteoclasts compared to BSA controls. Over 60% of the osteoclasts were aligned along the new bone tissue in the pulsatile PTH group, while most of the TRAP positive cells (over 85%) in the continuous PTH group were found distributed throughout the fibrous tissue inside the scaffold. The

osteoclast distribution in the local pulsatile and the systemic injection groups were similar, but local delivery recruited significantly more osteoclasts. Moreover, as the components of the devices were biodegradable and biocompatible polymers, the devices degraded/eroded over time and minimum immune reaction and inflammation were observed.

3.5 Systemic effect of local PTH delivery

Mouse tibiae from the different groups were examined using μCT to assess the potential systemic side effects of the local PTH releases. As expected, 3 weeks of PTH injection significantly increased trabecular bone volumes [27]. PTH released from the local device, both pulsatile and continuous, however, did not affect the trabecular bone, such that the volume of the trabecular bone remained unchanged compared to the BSA control group (Fig. 8 A, B). Serum was isolated at the end of the 3-week treatment regimen and ELISA analyses were employed to evaluate the levels of bone biomarkers. Serum P1NP (bone formation marker) and TRAP5b (bone resorption marker) suggested that the intermittent systemic injection of PTH increased systemic bone turnover, as the levels of P1NP and TRAP5b in the blood were significantly elevated compared to the local delivery groups (Fig. 8 C, D).

4. Discussion

PTH is the only FDA approved anabolic agent for the treatment of osteoporosis and its efficacy in stimulating bone remodeling, with net promotion of bone formation and few side effects, has been well established [18, 19, 28, 29]. The unique anabolic action of PTH implies its potential in bone regeneration, yet studies have been lacking in this type of administration for local regenerative application [20, 24, 30, 31].

In this study, we achieved bone defect repair using local pulsatile PTH delivery. The success of repurposing PTH from osteoporosis to bone regeneration was achieved by developing a novel long-term pulsatile PTH delivery device to accurately deliver PTH to the defect sites to induce local anabolic effects.

Current PTH treatment relies on systemic administration that was shown to be less effective in enhancing local defect repair and to have unintended systemic side effects. Local treatment, on the contrary, has advantages such as maintaining relatively higher local bioactive agent levels, need for reduced dose concentration or number of dosages, and circumventing possible adverse side effects resulting from systemic administration [32, 33].

The anabolic actions of PTH are also highly dependent on intermittent delivery and a specific temporal profile [24]. Current treatment requires daily injections, which is cumbersome for both patients and physicians. A self-regulated pulsatile delivery system capable of long-term delivery would be desirable. Despite that various delivery strategies have been developed, no successful and patient-friendly pulsatile system has been achieved [24]. Electrical controlled drug release microchips were fabricated to realize controlled PTH daily pulse release but such a device would require secondary surgery [34].

In the present study, patient-friendly drug delivery devices were utilized to expand PTH application and to determine optimal PTH release kinetics, pulsatile or continuous, in a local bone regeneration model. The pulsatile delivery device, made of alternating PA isolation layers and PTH drug layers, was preprogrammed to deliver daily PTH pulses for 21 days. The PTH/alginate blend was freeze-dried, cut into drug layers and then packed into the pulsatile device. This method enabled high drug loading efficiency and capacity and the bioactivity of the PTH was well preserved during the 3 weeks of PTH release. The continuous device, with identical shape and polymeric materials to that of pulsatile device, was loaded with the same amount of total PTH and delivered within the same time period (21 days). The difference between these two types of devices is the PTH distribution, where PTH is distributed in a layered structure to achieve pulsatile release or PTH is more uniformly distributed in the matrix within microspheres to achieve continuous release.

A highly porous NF scaffold was used to evaluate the two engineered PTH release modes for regeneration purpose. The PLLA scaffolds with NF surface feature were demonstrated to selectively enhance the adsorption of cell-adhesion proteins including fibronectin and vitronectin, increasing osteoblast adhesion [35]. Besides, such NF scaffolds enhance the osteoblastic differentiation of a variety of stem cells, including BMSCs, which are integral for bone defect healing [36, 37]. Here, the histological cross-section of the control group (scaffold with BSA delivery) also supported the conclusion that the NF structure alone could induce certain level of bone formation *in vivo* (Fig. 5 A, B). Furthermore, with different PTH release kinetics incorporated, distinct osteogenic outcomes in the NF scaffolds were observed. Local pulsatile PTH delivery significantly improved the defect repair, generating connected and robust new bone tissue throughout the scaffold, whereas local continuous delivery resulted in less bone in the NF scaffold versus the BSA control group.

From TRAP staining data (Fig. 5 C), we noticed that both PTH releases, pulsatile and continuous, were able to increase osteoclast numbers. Pulsatile PTH release induced stronger bone remodeling with enhanced numbers of the osteoclasts aligned along the formed bone tissue, while continuous PTH release resulted in reduced bone, with increased osteoclasts, not lining the bone, but throughout the fibrous tissue inside the scaffold. The results indicate that the local pulsatile PTH release was able to induce beneficial catabolic actions by stimulating osteoclasts to realize the needed bone remodeling activity in this specific bone-regeneration scenario.

It has been shown that 3 weeks of PTH systemic injection is also able to increase bone turnover and generate notable anabolic effects [25]. Thus, we also compared the local pulsatile PTH release device with the standard systemic PTH injection treatment, and found that local release was advantageous over the systemic injection in improving the defect repair. This local strategy may have benefitted from the more localized higher bioactive PTH level and the longer action time in the local defect sites. Given the 8 min half-life of PTH [38], only a part of the total bioactive PTH could reach the defect sites considering the bioactivity loss during circulation time when PTH is given systemically. On the contrary, the local delivery strategy is more likely to maintain bioactive PTH level within an effective range for a period of time.

In addition to enhancing local defect repair, local PTH releases led to little undesired systemic effects, whereas PTH systemic injection resulted in clear systemic effects as expected. μCT and serum data showed that PTH injection significantly increased tibiae trabecular bone volume and serum bone formation biomarkers, while PTH local release did not affect tibiae trabecular bone and exerted only minor effects on serum bone formation biomarkers. These results indicate that PTH release from the device was likely to be delivered and act more locally.

The polymeric materials used in this system, PLLA, PA, PCL and alginate, have been used as components of FDA-approved devices for certain medical applications [39]. The biodegradable and biocompatible devices developed in this study elicited minimum immune response and inflammation, which are particularly advantageous for the defect repair application. In addition, this approach needs only a one-time administration (implantation) instead of daily injection for 3 weeks and there is no need for retrieval of the empty devices after the drug release is complete. Therefore, the implantable device is more patient-friendly and is promising for clinical translation.

5. Conclusion

In summary, PTH, a FDA-approved anabolic agent for osteoporosis, was repurposed to repair local bone defects. Current PTH treatment requires daily injection, while in this work PTH was incorporated into a novel biodegradable device, which was capable of delivering PTH to the defect area in a preprogrammed pulsatile manner. It was found that local continuous PTH release inhibited, while local pulsatile PTH release promoted bone regeneration. In addition, the local pulsatile delivery strategy significantly improved the osteogenic outcome and reduced the systemic side effects compared to the standard PTH injection treatment. This acellular therapy provides a novel strategy to improve bone defect repair by integrating a biomimetic scaffold and an anabolic local delivery strategy to maximize the regenerative effects within the intended areas of interest. This biomaterial technology holds promise for bone defect regeneration without addition of external cells, the burden of daily PTH injections, or the need for device removal surgery. The technology could also be readily employed to deliver other therapeutics or their combinations in a tailored manner to maximize their therapeutic effects.

Acknowledgments

This work was supported by the US DOD (W81XWH-12-2-0008) and the National Institutes of Health (DE022327 and DK53904).

References

1. Ma PX. Biomimetic materials for tissue engineering. Advanced Drug Delivery Reviews. 2008; 60:184–98. [PubMed: 18045729]
2. Holzwarth JM, Ma PX. Biomimetic nanofibrous scaffolds for bone tissue engineering. Biomaterials. 2011; 32:9622–9. [PubMed: 21944829]
3. Zhang X, Li Y, Chen YE, Chen J, Ma PX. Cell-free 3D scaffold with two-stage delivery of miRNA-26a to regenerate critical-sized bone defects. Nat Commun. 2016:7.

4. Neuss S, Apel C, Buttler P, Denecke B, Dhanasingh A, Ding X, et al. Assessment of stem cell/biomaterial combinations for stem cell-based tissue engineering. Biomaterials. 2008; 29:302–13. [PubMed: 17935776]
5. Bueno EM, Glowacki J. Cell-free and cell-based approaches for bone regeneration. Nat Rev Rheumatol. 2009; 5:685–97. [PubMed: 19901916]
6. Chan BP, Leong KW. Scaffolding in tissue engineering: general approaches and tissue-specific considerations. European Spine Journal. 2008; 17:467–79. [PubMed: 19005702]
7. Woo KM, Jun J-H, Chen VJ, Seo J, Baek J-H, Ryoo H-M, et al. Nano-fibrous scaffolding promotes osteoblast differentiation and biomineralization. Biomaterials. 2007; 28:335–43. [PubMed: 16854461]
8. Wei G, Jin Q, Giannobile WV, Ma PX. The enhancement of osteogenesis by nano-fibrous scaffolds incorporating rhBMP-7 nanospheres. Biomaterials. 2007; 28:2087–96. [PubMed: 17239946]
9. Balmayor ER. Targeted delivery as key for the success of small osteoinductive molecules. Advanced Drug Delivery Reviews. 2015; 94:13–27. [PubMed: 25959428]
10. Lo KWH, Ulery BD, Kan HM, Ashe KM, Laurencin CT. Evaluating the feasibility of utilizing the small molecule phenamil as a novel biofactor for bone regenerative engineering. Journal of Tissue Engineering and Regenerative Medicine. 2014; 8:728–36. [PubMed: 22815259]
11. Chew SY, Wen J, Yim EKF, Leong KW. Sustained Release of Proteins from Electrospun Biodegradable Fibers. Biomacromolecules. 2005; 6:2017–24. [PubMed: 16004440]
12. Wang W, Dang M, Zhang Z, Hu J, Eyster TW, Ni L, et al. Dentin regeneration by stem cells of apical papilla on injectable nanofibrous microspheres and stimulated by controlled BMP-2 release. Acta Biomaterialia. 2016; 36:63–72. [PubMed: 26971664]
13. Kofron MD, Laurencin CT. Bone tissue engineering by gene delivery. Advanced Drug Delivery Reviews. 2006; 58:555–76. [PubMed: 16790291]
14. Ito H, Koefoed M, Tiyapatanaputi P, Gromov K, Goater JJ, Carmouche J, et al. Remodeling of cortical bone allografts mediated by adherent rAAV-RANKL and VEGF gene therapy. Nat Med. 2005; 11:291–7. [PubMed: 15711561]
15. Pashuck ET, Stevens MM. Designing Regenerative Biomaterial Therapies for the Clinic. Science Translational Medicine. 2012; 4:160sr4-sr4.
16. Dempster DW, Cosman F, Kurland ES, Zhou H, Nieves J, Woelfert L, et al. Effects of Daily Treatment with Parathyroid Hormone on Bone Microarchitecture and Turnover in Patients with Osteoporosis: A Paired Biopsy Study*. Journal of Bone and Mineral Research. 2001; 16:1846–53. [PubMed: 11585349]
17. Neer RM, Arnaud CD, Zanchetta JR, Prince R, Gaich GA, Reginster J-Y, et al. Effect of Parathyroid Hormone (1–34) on Fractures and Bone Mineral Density in Postmenopausal Women with Osteoporosis. New England Journal of Medicine. 2001; 344:1434–41. [PubMed: 11346808]
18. Dempster DW, Cosman F, Parisien MAY, Shen V, Lindsay R. Anabolic Actions of Parathyroid Hormone on Bone. Endocrine Reviews. 1993; 14:690–709. [PubMed: 8119233]
19. Qin L, Raggatt LJ, Partridge NC. Parathyroid hormone: a double-edged sword for bone metabolism. Trends in Endocrinology & Metabolism. 2004; 15:60–5. [PubMed: 15036251]
20. Chan HL, McCauley LK. Parathyroid Hormone Applications in the Craniofacial Skeleton. Journal of Dental Research. 2013; 92:18–25. [PubMed: 23071071]
21. Hou S, McCauley LK, Ma PX. Synthesis and Erosion Properties of PEG-Containing Polyanhydrides. Macromolecular Bioscience. 2007; 7:620–8. [PubMed: 17457940]
22. Wei G, Ma PX. Macroporous and nanofibrous polymer scaffolds and polymer/bone-like apatite composite scaffolds generated by sugar spheres. Journal of Biomedical Materials Research Part A. 2006; 78A:306–15.
23. Wei G, Pettway GJ, McCauley LK, Ma PX. The release profiles and bioactivity of parathyroid hormone from poly(lactic-co-glycolic acid) microspheres. Biomaterials. 2004; 25:345–52. [PubMed: 14585722]
24. Liu X, Pettway GJ, McCauley LK, Ma PX. Pulsatile release of parathyroid hormone from an implantable delivery system. Biomaterials. 2007; 28:4124–31. [PubMed: 17576005]

25. Pettway GJ, Schneider A, Koh AJ, Widjaja E, Morris MD, Meganck JA, et al. Anabolic actions of PTH (1–34): Use of a novel tissue engineering model to investigate temporal effects on bone. Bone. 2005; 36:959–70. [PubMed: 15878317]
26. Leong KW, D'Amore P, Marletta M, Langer R. Bioerodible polyanhydrides as drug-carrier matrices. II. Biocompatibility and chemical reactivity. Journal of Biomedical Materials Research. 1986; 20:51–64. [PubMed: 3949823]
27. Koh AJ, Novince CM, Li X, Wang T, Taichman RS, McCauley LK. An Irradiation-Altered Bone Marrow Microenvironment Impacts Anabolic Actions of PTH. Endocrinology. 2011; 152:4525–36. [PubMed: 22045660]
28. Andreassen TT, Ejersted C, Oxlund H. Intermittent Parathyroid Hormone (1–34) Treatment Increases Callus Formation and Mechanical Strength of Healing Rat Fractures. Journal of Bone and Mineral Research. 1999; 14:960–8. [PubMed: 10352105]
29. Poole KES, Reeve J. Parathyroid hormone — a bone anabolic and catabolic agent. Current Opinion in Pharmacology. 2005; 5:612–7. [PubMed: 16181808]
30. Nardi A, Ventura L, Cozzi L, Tonini G, Zennaro R, Celi M, et al. The bone anabolic therapy. Aging Clinical and Experimental Research. 2013; 25:121–4.
31. Dhillon RS, Schwarz EM. Teriparatide Therapy as an Adjuvant for Tissue Engineering and Integration of Biomaterials. Journal of materials research. 2011; 4:1117–31. [PubMed: 21857768]
32. Zhang S, Ermann J, Succi MD, Zhou A, Hamilton MJ, Cao B, et al. An inflammation-targeting hydrogel for local drug delivery in inflammatory bowel disease. Science Translational Medicine. 2015; 7:300ra128–300ra128.
33. Zhang Z, Hu J, Ma PX. Nanofiber-based delivery of bioactive agents and stem cells to bone sites. Advanced Drug Delivery Reviews. 2012; 64:1129–41. [PubMed: 22579758]
34. Farra R, Sheppard NF, McCabe L, Neer RM, Anderson JM, Santini JT, et al. First-in-Human Testing of a Wirelessly Controlled Drug Delivery Microchip. Science Translational Medicine. 2012; 4:122ra21–ra21.
35. Woo KM, Chen VJ, Ma PX. Nano-fibrous scaffolding architecture selectively enhances protein adsorption contributing to cell attachment. Journal of Biomedical Materials Research Part A. 2003; 67A:531–7.
36. Smith LA, Liu X, Hu J, Ma PX. The influence of three-dimensional nanofibrous scaffolds on the osteogenic differentiation of embryonic stem cells. Biomaterials. 2009; 30:2516–22. [PubMed: 19176243]
37. Hu J, Liu X, Ma PX. Induction of osteoblast differentiation phenotype on poly(l-lactic acid) nanofibrous matrix. Biomaterials. 2008; 29:3815–21. [PubMed: 18617260]
38. Calò PG, Pisano G, Loi G, Medas F, Barca L, Atzeni M, et al. Intraoperative parathyroid hormone assay during focused parathyroidectomy: the importance of 20 minutes measurement. BMC Surgery. 2013; 13:1–5. [PubMed: 23356494]
39. Nair LS, Laurencin CT. Biodegradable polymers as biomaterials. Progress in Polymer Science. 2007; 32:762–98.

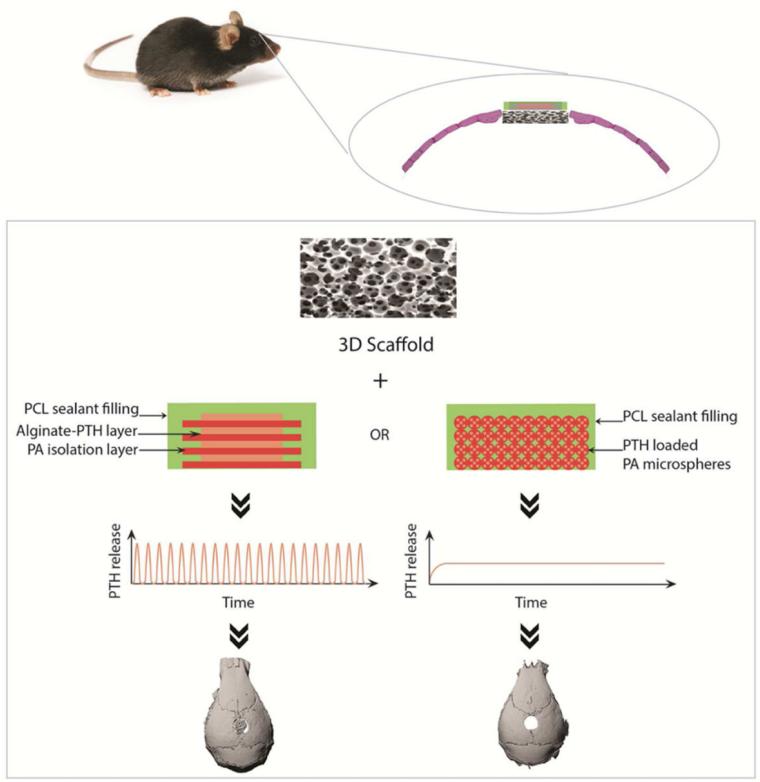

Figure 1.

Experimental design of using a 3D cell-free scaffold and a PTH deliver device (pulsatile or continuous) to repair calvarial bone defect in a mouse model.

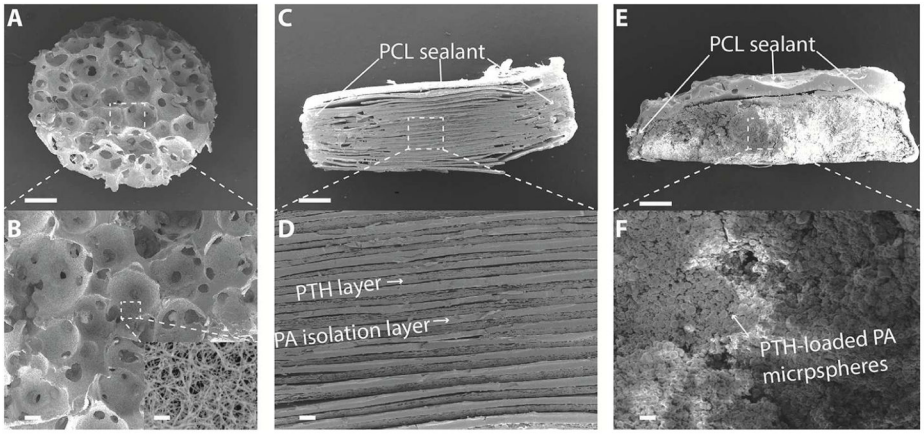

Figure 2.

Scanning electron microscopy (SEM) images of scaffold and PTH delivery devices. (A, B) Nanofibrous PLLA scaffold with interconnected spherical pore network; (C, D) the pulsatile PTH release device; and (E, F) the continuous PTH release device. Scale bars: 400 μm in A, C, E and 50 μm in B, D, F. Inset in Figure 2 B shows the nanofiberous architecture of the scaffold at a higher magnification (scale bar: 2 μm).

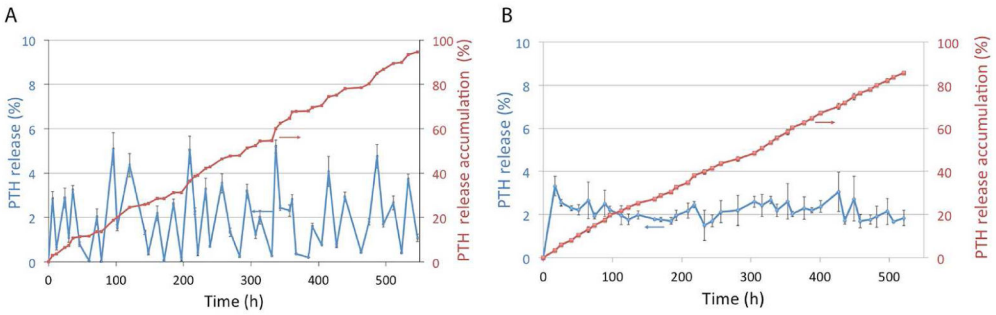

Figure 3.

In vitro drug release profiles. (A) 21-day PTH release from the pulsatile device; (B) 21-day PTH release from the continuous device. The red curves were the cumulative PTH release curves measured using a PTH ELISA kit (n=3).

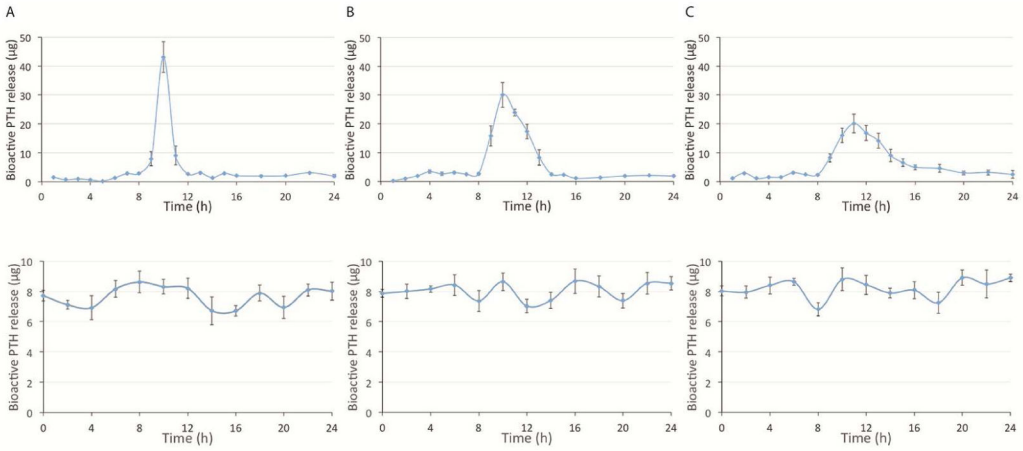

Figure 4.

In vitro bioactive PTH release curves from the two different delivery devices. cAMP-binding assays were used to determine the bioactive PTH amounts released from a pulsatile device (upper panel) and a continuous device (lower panel) at 3 time points: (A) day 1, (B) day 10, and (C) day 20 (n=3).

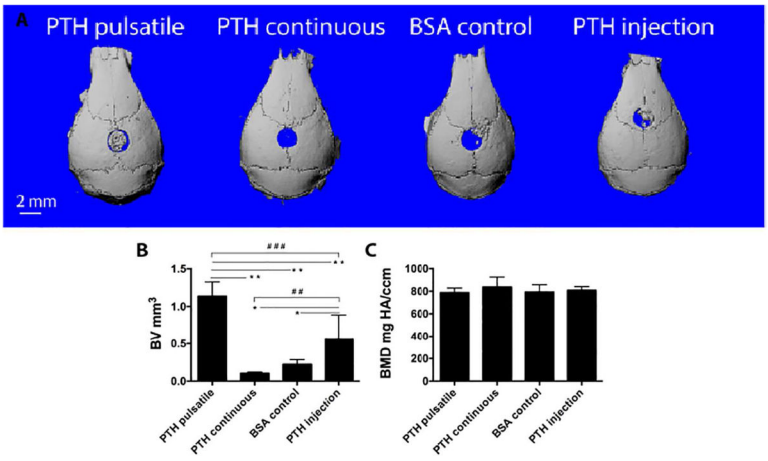

Figure 5.

μCT characterization of the local defect repair in 8 weeks. (A) Representative μCT reconstructions of mouse calvarial defects in different PTH delivery groups. (B) The new bone volume; and (C) The new bone mineral density. n=6~9 per group, *P<0.05, **P<0.005, #P<0.05, ##P<0.005, ###P<0.001.

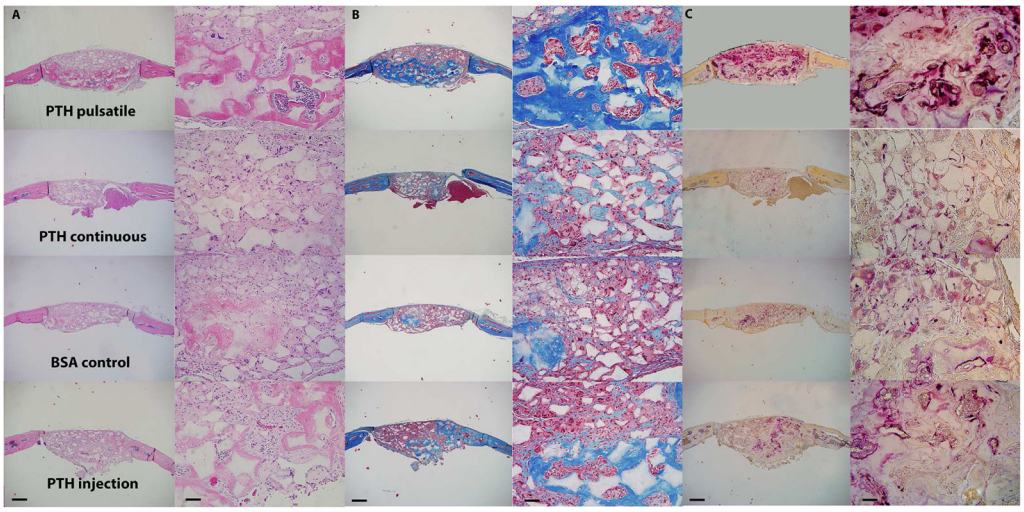

Figure 6.

Histological characterization of the bone defect repair 8 weeks after implantation. (A) H&E staining, (B) Trichrome staining, and (C) TRAP staining of different PTH delivery groups. Scale bars: 0.5mm in the left column and 0.2mm in the right column.

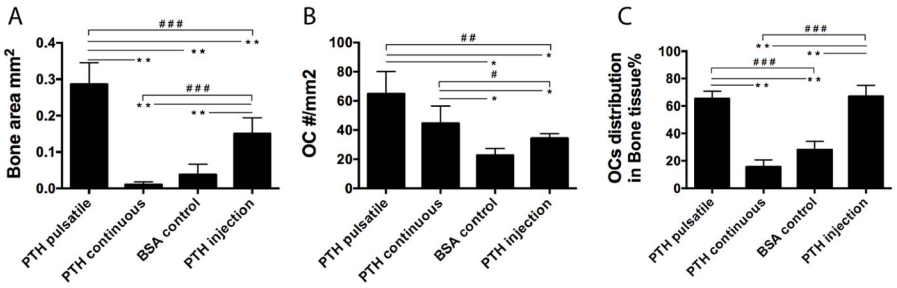

Figure 7.

Quantitative analysis of the bone repair using histomorphometry. (A) Newly formed bone areas, (B) TRAP positive osteoclasts numbers, and (C) the distribution of the osteoclasts in the bone area and scaffold area quantified using histomorphometry. n=6~9 per group, *P<0.05, **P<0.005, #P<0.05, ##P<0.005, ###P<0.001.

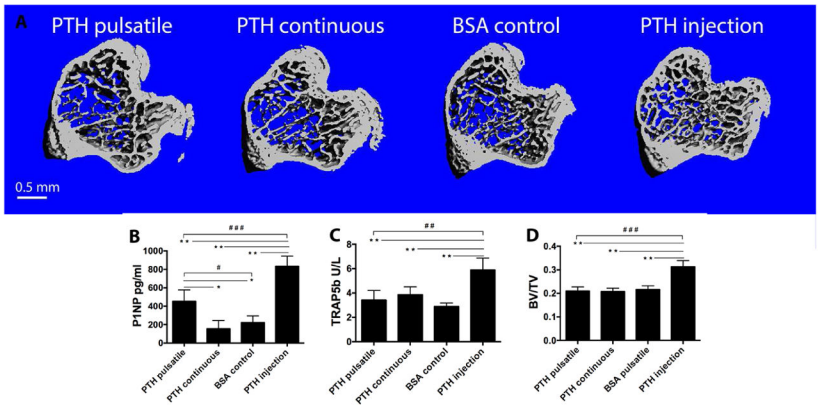

Figure 8.

Analysis of the systemic effects of PTH release from the local delivery devices. (A) Representative μCT reconstructions of the tibiae from different treatment groups; (B) Trabecular bone volume; (C) Serum P1NP level and (D) TRAP5b level measured using ELISA kits. n=6~9 per group, *P<0.05, **P<0.005, #P<0.05, ##P<0.005, ###P<0.001.